


SCIENTIFIC REPORTS



OPEN

A Bowman-Birk type chymotrypsin inhibitor peptide from the amphibian, *Hylarana erythraea*

Luyao Zhang, Xiaoling Chen, Yue Wu, Mei Zhou, Chengbang Ma, Xinping Xi , Tianbao Chen, Brian Walker, Chris Shaw & Lei Wang

The first amphibian skin secretion-derived Bowman-Birk type chymotrypsin inhibitor is described here from the Asian green frog, *Hylarana erythraea*, and was identified by use of molecular cloning and tandem mass spectrometric amino acid sequencing. It was named *Hylarana erythraea* chymotrypsin inhibitor (HECI) and in addition to inhibition of chymotrypsin ($K_i = 3.92 \pm 0.35 \mu\text{M}$), the peptide also inhibited the 20S proteasome ($K_i = 8.55 \pm 1.84 \mu\text{M}$). Additionally, an analogue of HECI, named K⁹-HECI, in which Phe⁹ was substituted by Lys⁹ at the P1 position, was functional as a trypsin inhibitor. Both peptides exhibited anti-proliferation activity against the human cancer cell lines, H157, PC-3 and MCF-7, up to a concentration of 1 mM and possessed a low degree of cytotoxicity on normal cells, HMEC-1. However, HECI exhibited higher anti-proliferative potency against H157. The results indicate that HECI, inhibiting chymotryptic-like activity of proteasome, could provide new insights in treatment of lung cancer.

Serine protease inhibitors are important in many crucial physiological processes within the human body¹. Among three serine inhibitor families, the Bowman-Birk inhibitors (BBI) found in plants and amphibians, have been studied because of their potent protease inhibition. There are two groups of BBIs - one consists of large proteins which have more than one reactive site² and the other consists of short looped peptides normally containing less than 20 residues with higher specific activity³.

Most amphibian-derived BBI peptides have been isolated from skin secretions of frogs from the family Ranidae, including *Lithobates pipiens* (pLR), *Lithobates sevosus* (pYR), *Odorrana versabilis* (HV-BBI), *Odorrana hejiangensis* (HJTI), *Hylarana latouchii* (pLR-HL) and *Odorrana schmackeri* (OSTI)⁴⁻⁹. These BBI peptides contain 17 to 18 amino acid residues, possess a common conserved internal sequence motif -WTKSXPPXP- and a single intramolecular disulphide bond which presents the conserved reactive loop¹⁰. They possess inhibitory activity with K_i values in the micromolar range^{5-7,9,11}. Also, several BBI peptides are also highly potent trypsin inhibitors⁶ and others play important roles in the regulation of immune responses^{4,12}.

Some BBI proteins such as the MSTI from snail medic seeds, BTCI from Black-eyed pea and a trypsin inhibitor from Hokkaido large black soybeans have anti-proliferative effects on tumour cells¹³⁻¹⁵. Several reports suggested that the anti-carcinogenic functions of serine protease inhibitors are probably related to their chymotrypsin-like and trypsin-like inhibitions on 20S proteasome¹⁵⁻¹⁷. The inhibition of 20S proteasome may suppress the proliferation of cancer cells through preventing the degradation of pro-apoptotic factors and inhibiting the activation of NF κ B¹⁸.

Here, the discovery of the first chymotrypsin inhibitory BBI peptide from an amphibian skin secretion, is described from the Asian green frog, *Hylarana erythraea*. The peptide was isolated by RP-HPLC fractionation by nature of its chymotrypsin inhibitory activity determined by preliminary activity screening. The amino acid sequence was determined as TVLRGCWTFSPFKPCI-amide, by Edman degradation and further confirmed by MS/MS fragmentation. An analogue (K⁹-HECI, TVLRGCWTKSFPPKPCI-amide) which was used for BBI inhibitor P1 position analysis, was synthesized in parallel with HECI.

Natural Drug Discovery Group, School of Pharmacy, Queen's University, Belfast, BT9 7BL, Northern Ireland, UK. Luyao Zhang and Xiaoling Chen contributed equally to this work. Correspondence and requests for materials should be addressed to C.M. (email: c.ma@qub.ac.uk) or X.X. (email: x.xi@qub.ac.uk)

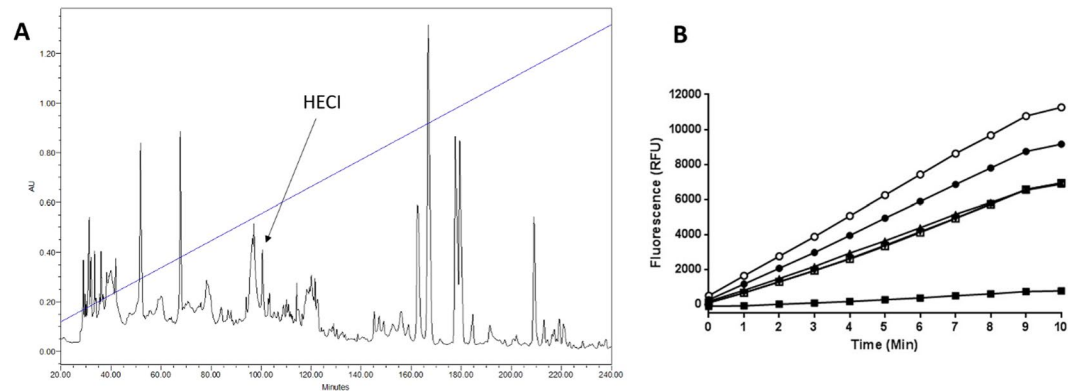


Figure 1. Identification and structural analysis of HECI. (A) RP-HPLC chromatogram of *Hyalarana erythraea* skin secretion. The linear gradient of buffer B (0.05/19.95/80.0 (v/v/v) TFA/water/acetonitrile) is indicated in blue line. The arrow indicates the retention time of HECI, about 34% acetonitrile. (B) Chymotrypsin inhibition activity screening of HPLC fractions 98–102 min (○ 98 min, ● 99 min, ■ 100 min, □ 101 min, ▲ 102 min).

#1	b(1+)	b(2+)	Seq.	y(1+)	y(2+)	#2
1	102.055	51.531	T			17
2	201.123	101.065	V	1849.961	<u>925.484</u>	16
3	314.207	157.607	L	1750.892	<u>875.950</u>	15
4	<u>470.309</u>	235.658	R	<u>1637.808</u>	819.408	14
5	<u>527.330</u>	264.169	G	<u>1481.707</u>	741.357	13
6	<u>630.339</u>	<u>315.673</u>	C	<u>1424.685</u>	<u>712.846</u>	12
7	<u>816.419</u>	408.713	W	<u>1321.676</u>	661.342	11
8	<u>917.466</u>	459.237	T	<u>1135.597</u>	568.302	10
9	<u>1064.535</u>	<u>532.771</u>	F	1034.549	517.778	9
10	<u>1151.567</u>	576.287	S	<u>887.481</u>	444.244	8
11	<u>1298.635</u>	<u>649.821</u>	F	<u>800.449</u>	400.728	7
12	<u>1395.688</u>	<u>698.348</u>	P	<u>653.380</u>	<u>327.194</u>	6
13	<u>1492.741</u>	<u>746.874</u>	P	<u>556.328</u>	<u>278.668</u>	5
14	<u>1620.836</u>	<u>810.921</u>	K	459.275	230.141	4
15	1717.888	<u>859.448</u>	P	<u>331.180</u>	166.094	3
16	1820.898	<u>910.952</u>	C	234.127	117.567	2
17	—	—	I-Amidated	131.118	66.063	1

Table 1. MS/MS fragmentation sequencing data of HECI. Through CID collision, the parent ion was fragmented into singly/doubly charged ions. The observed m/z ratios of b-ions y-ions are single-underlined.

Results

Identification and structural analysis of HECI. The skin secretion of *Hyalarana erythraea* was fractionated by RP-HPLC over 240 min in the gradient from 0% to 100% buffer B (0.05/19.95/80.0 (v/v/v) TFA/water/acetonitrile) (Fig. 1A). Each fraction was reconstituted in PBS and subjected to the chymotrypsin inhibition assay and fraction # 100 was found to exhibit significant chymotrypsin inhibitory activity (Fig. 1B). The MS full-scan analysis of this fraction revealed the presence of a single molecule with a molecular mass of 1949.6 Da. Subsequent Edman degradation of this peptide found it to be composed of 17 amino acid residues - TVLRGCWTFSPKPCI - with a C-terminal amidation. MS/MS fragmentation confirmed the sequence as: TVLRGCWTFSPKPCI-NH₂ (Table 1), and this novel BBI peptide was named *Hyalarana erythraea* chymotrypsin inhibitor (HECI).

Molecular cloning of the HECI precursor-encoding cDNA from a skin secretion-derived cDNA library of *Hyalarana erythraea*.

A single transcript encoding the biosynthetic precursor of the novel peptide named, HECI, was repeatedly cloned from the library. From this, both the nucleotide and translated open reading frame amino acid sequence of the HECI precursor were successfully determined (Fig. 2A). The biosynthetic precursor of HECI consisted of 63 amino acids organized as a putative signal peptide domain of 22 residues, which was followed by a 21-mer acidic amino acid residue-rich “spacer” peptide. The mature peptide sequence followed a typical processing site (-KR-) and ended in a Gly residue, which is a classical amide donor for C-terminal amidation. The alignments of the prepeptides and the cDNAs of amphibian skin-derived BBI peptides showed that they exhibited high degrees of similarity. The signal peptide domain and the inhibitory motif within the mature peptides, were both highly-conserved (Fig. 2B and C). The loop structure of the HECI

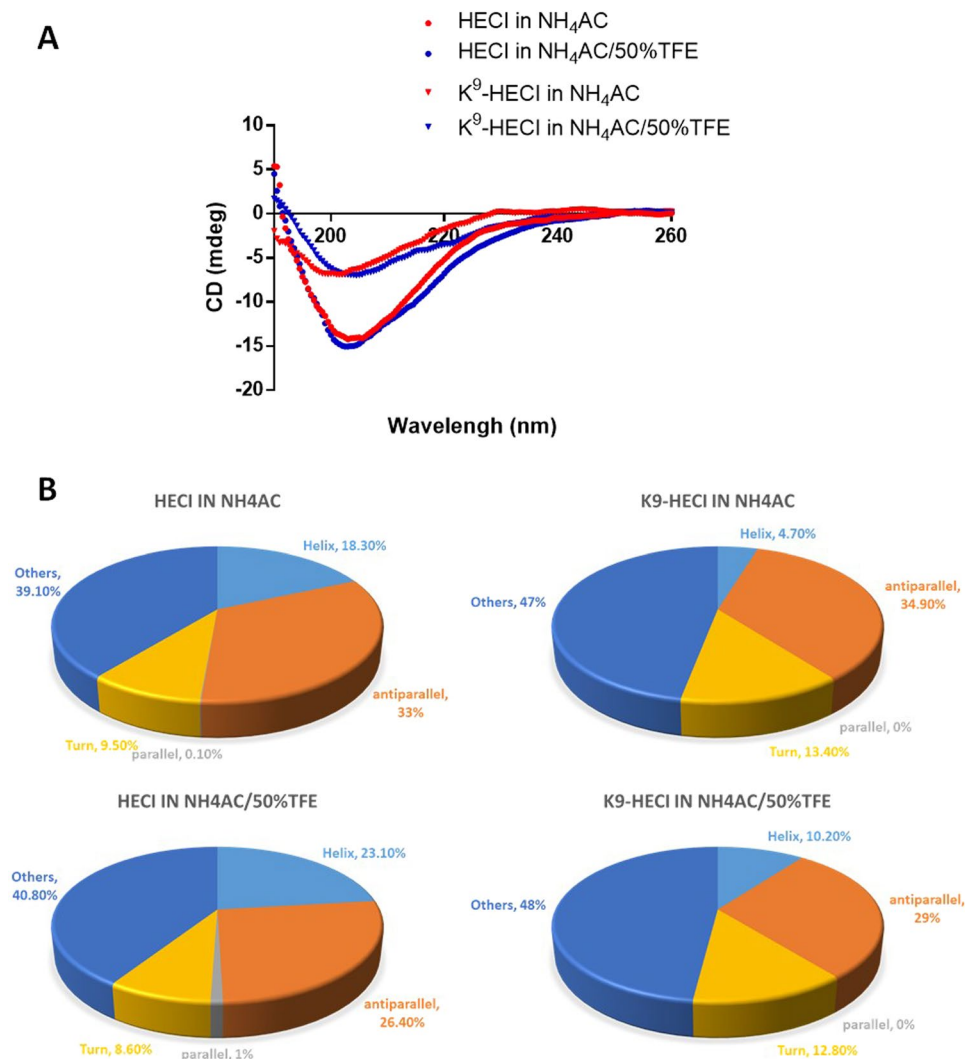


Figure 3. Secondary structure analyses of HECl and K⁹-HECl. **(A)** The CD spectra of HECl (dot) and K⁹-HECl (triangle) were measured in aqueous NH₄AC buffer (red colour) and membrane-mimic NH₄AC/50%TFE buffer (blue colour), respectively. **(B)** The proportion of different secondary structures domain were predicted and calculated using the online software, BeStSel³⁵.

against chymotrypsin. Here, we report the first example of a natural chymotrypsin inhibitory BBI peptide, named HECl, from the skin secretion of the Asian green frog, *Hylarana erythraea*.

The signal peptide sequence and cDNA sequence of the biosynthetic precursor of this natural peptide are similar to those encoding other BBI peptides from amphibian skin secretions. However, the amino acids at P1 and P2' positions of HECl are both Phe residues, which is consistent with observed chymotrypsin inhibition in this peptide and in other such BBIs¹⁹. As expected, HECl showed moderate chymotrypsin inhibitory activity similar to that observed for P1 Phe-substituted analogues of amphibian skin-derived trypsin inhibitory BBI peptides^{5–7,9,11}. Hence, the peptide analogue K⁹-HECl was designed and synthesized to determine if trypsin inhibition activity could be reverse engineered. Interestingly, K⁹-HECl was found to have both trypsin and chymotrypsin inhibitory activities, therefore we deduced that the P2' position was also a key position for inhibition specificity of short BBI peptides. This hypothesis differs with respect to the function of P2' sites in large BBI proteins, which are related to the peptide hydrolysis rate²⁰.

Several previous reports have shown that chymotrypsin inhibitors generally also have partial inhibitory activities on the proteasome⁸. Thus, a proteasome inhibition test on HECl was performed. The result showed that HECl had moderate inhibition on the chymotrypsin-like active site of the human 20 S proteasome. Indeed, the highest concentration of HECl even showed a more effective inhibition of the 20 S proteasome than it did on chymotrypsin. Additionally, the time of HECl inhibition of the 20 S proteasome was longer than that observed for chymotrypsin, which might be explained by the higher affinity of HECl for the 20 S proteasome. As we know, 20 S proteasome consists of 28 subunits, three of which conduct the tryptic (β 2), chymotryptic (β 5) and caspase-like (β 1) activities, respectively²¹. Whilst, the catalytic nucleophile of proteasome subunits is the highly-conserved N-terminal threonine²². Inhibition of proteasome activities and subunit-specific amino-terminal threonine

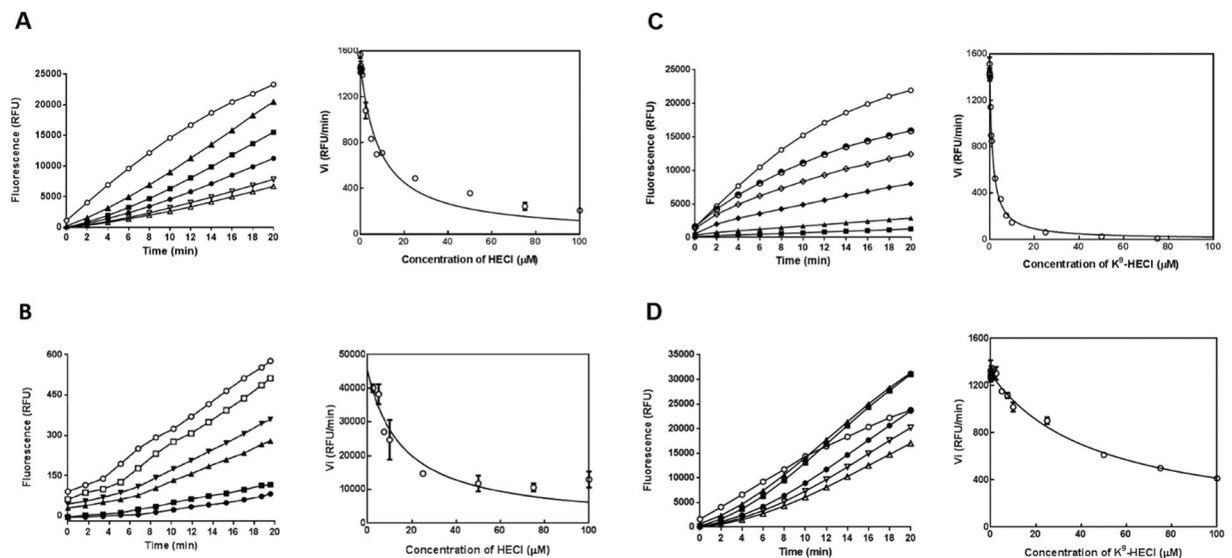


Figure 4. Inhibitory activity of HECI and the Lys-substituted analogue on trypsin, chymotrypsin and the 20S proteasome. **(A)** Progress curves and corresponding Morrison plot for chymotrypsin proteolysis in the presence of different concentrations of HECI. **(B)** Progress curves and corresponding Morrison plot for human proteasome 20 S proteolysis in the presence of different concentrations of HECI. **(C)** Progress curves and corresponding Morrison plot for trypsin proteolysis in the presence of different concentrations of K⁹-HECI. **(D)** Progress curves and corresponding Morrison plot for chymotrypsin proteolysis in the presence of different concentrations of K⁹-HECI. (\triangle 100 μ M, ∇ 75 μ M, \bullet 50 μ M, \blacksquare 25 μ M, \blacktriangle 10 μ M, \blacktriangledown 7.5 μ M, \square 5 μ M, \blacklozenge 2.5 μ M, \diamond 1 μ M, \bullet 0.25 μ M, \circ 0 μ M).

modification by lactacystin²³, differing from the conventional serine in the active site, which may explain the different affinity of HECI between chymotrypsin and 20 S proteasome β 5 subunit. As the 20 S proteasome plays a critical role in regulating many processes in the cell that are important for cancer cell growth and survive, and it mainly involves the chymotrypsin-like activity²⁴. We therefore assumed that HECI might have anticancer properties, which indeed were confirmed in this study.

The major hypothesis of anti-cancer activity of peptides possessing chymotrypsin inhibition is that the peptide might be translocated into the cell and react with the related intracellular enzymes like the 20 S proteasome. Also, recent research support the idea that the anti-carcinogenic functions of some BBIs might be related to their proteasome inhibition²⁵. Although both peptides inhibited the growth of three cancer cells up to the highest concentration, HECI shows more potent activity against the non-small cell lung cancer, H157 than the others. Indeed, proteasome inhibitor has been proved to inhibit a range of cancer cell lines but much more potent against H460, another non-small cell lung cancer¹⁸, which might be related to the NF- κ B-mediated antiapoptotic pathway in non-small cell lung cancer²⁶ that decreased the level of Bcl-2 to directly associate with apoptosis²⁷. Interestingly, both peptides showed similar degree of inhibition at 1 mM on each cancer cell lines. In this study, we only investigated the chymotryptic-like activity of proteasome instead of all the catalytic sites, though the K⁹-HECI might be able to inhibit the tryptic-like β 5 subunit. Previous study showed that plant-derived BBI, processing the inhibitory activity on those three subunits, inhibited the MCF-7 by means of apoptosis¹⁵, indicating that inhibition of all the subunits could contribute to the apoptosis-induced ability. Obviously, a lower anti-proliferation inhibitory activity of K⁹-HECI was observed that confirmed the chymotrypsin-like subunit produces the lead effect on anti-proliferation of cancer cells^{15,28,29}. That the similar potency of both peptides on MCF-7 but the distinct activity on H157 and PC-3 also suggests different apoptosis pathways might be associated with proteasome inhibition. Additionally, considering that membrane transport is required of the peptide, more investigations would be needed to assess the transmembrane permeation capabilities of HECI.

Meanwhile, some amphibian skin derived BBIs exhibited antimicrobial activity, which was reported to insert into the hydrophobic core of membrane to form transmembrane pores³⁰. The amphipathic peptide can increase the membrane permeability that results in the co-delivery of complex molecules from amphibian skin secretion³¹. It is possible that both peptides could compromise the cell membrane, resulting in the inhibition of cell proliferation. Additionally, the CD spectra show that HECI has 2-fold greater helix content than K⁹-HECI in a membrane-mimic environment. When the HECI attaches to the cell membrane, it could be more efficient in interacting with the cell membrane than K⁹-HECI due to its higher hydrophobicity as a consequence of the highly hydrophobic region (-WTFSPF-) of HECI^{32,33}. When increasing the concentration to 1 mM, both peptides, losing specificity, showed similar potency against all cancer cells, which could be explained by the non-specific membrane permeabilization.

However, both HECI and K⁹-HECI showed only slight cytotoxicity on HMEC-1 and low degree of haemolysis of mammalian erythrocytes, which suggested that both proteasome inhibition and membrane permeabilization would occur in the antiproliferative activity on cancer cells, but the cell apoptosis through inhibition

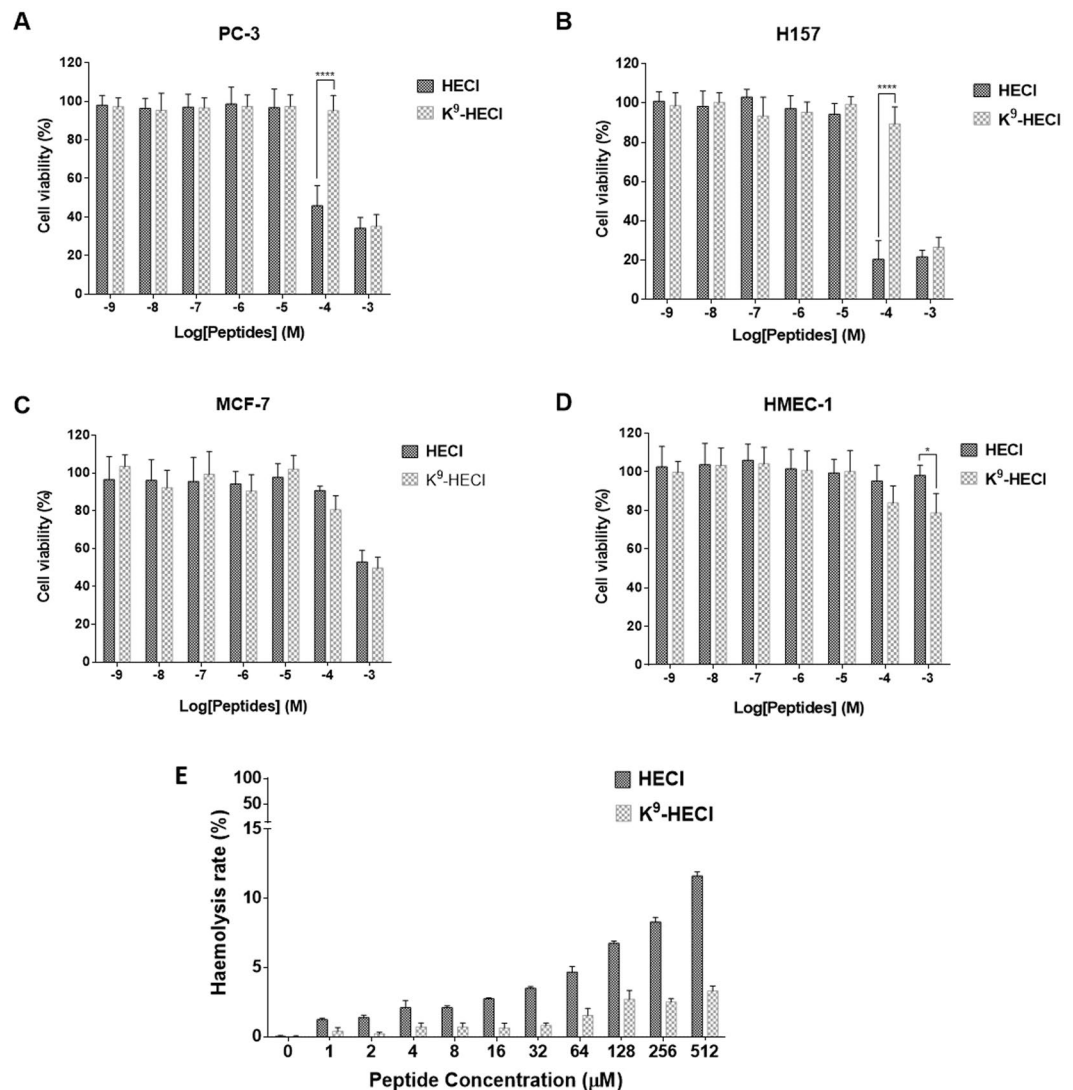


Figure 5. Effects of HECI and the Lys-substituted analogue on cancer cell lines, a normal cell line and erythrocytes. Cell viability of cancer cell line (A) PC-3, (B) H157, (C) MCF-7 and (D) the normal cell line HMEC-1 at different concentrations of HECI (dark grey) and K⁹-HECI (light grey). Statistical significance of difference was analysed by two-way ANOVA (* $p < 0.05$, **** $p < 0.0001$). (E) Haemolysis rates of HECI and K⁹-HECI on erythrocytes after being incubated for 4h. The sample for the 0 μ M control group was PBS only.

of proteasome might be predominant. Additionally, both peptides exhibited low degree of cytotoxicity on the normal cell line, indicating that it might be able to specifically target cancer cells, especially H157. The reason behind this is not clear so far, but an explanation of the low cytotoxicity on normal cells is that the expression level of proteasome inhibitor could be at a much lower level in normal cells, but higher in cancer cells³⁴.

In summary, this is the first report of a chymotrypsin inhibitory BBI peptide in amphibian skin secretion, from the Asian frog, *Hylarana erythraea*. The peptide possesses inhibitory activities on chymotrypsin and the 20S proteasome and its P1 Lys-substituted analogue showed potent trypsin inhibitory activity. HECI also showed more potent anticancer activity against PC-3 and H157 cell lines with low degree of cytotoxicity against normal cell lines. This study of HECI has provided a new insight into the possible clinical applications of skin-derived BBI peptides as well as their roles as potential candidates for natural drug development.

Methods

Acquisition of *Hylarana erythraea* skin secretion. The skin secretions of four *Hylarana erythraea* frogs were obtained by gentle electrical stimulation and hand massaging, which was described in detail previously (Tyler *et al.*, 1992). Briefly, the moist frog dorsal skin was stimulated by 3–5 V, 100 Hz, AC. Then the electrode was moved slowly on the skin which was covered by glands for 10 s. Finally, the white secretion was washed off by deionized water and immediately snap frozen in liquid nitrogen. The samples were lyophilized for future analysis. The study was performed according to the guidelines in the UK Animal (Scientific Procedures) Act 1986,

project license PPL 2694, issued by the Department of Health, Social Services and Public Safety, Northern Ireland. Procedures had been vetted by the IACUC of Queen's University Belfast, and approved on 1st March, 2011.

Initially fractionation of skin secretion. Five milligrams of lyophilized skin secretion were dissolved in 1 ml of deionized water containing 0.05% (v/v) trifluoroacetic acid (TFA, obtained from Sigma-Aldrich, St. Louis, MO, USA). The sample was subsequently centrifuged and the supernatant was further filtered through a 0.45 μ m RC membrane (Phenomenex, Macclesfield, UK). The filtrate was injected into a reverse-phase HPLC system (UV Detector: Waters 2489; Binary HPLC Pump: Waters 1525; Autosampler: Waters 2707 (Waters Ireland, Dublin, Ireland); Column: Phenomenex Aeris Peptide, C18, 250 \times 10.0 mm (Phenomenex, Macclesfield, UK), followed by elution with a gradient program from 0.05/99.95 (v/v) TFA/water (0 min) to 0.05/19.95/80.0 (v/v/v) TFA/water/ acetonitrile in 240 min. The column effluent was monitored by UV absorbance at 214 nm, and fractions were collected automatically at 1 min intervals.

Chymotrypsin inhibition assay screen. HPLC fractions were dried by Eppendorf Concentrator plus (Eppendorf, Hamburg, Germany) in the alcohol/vacuum mode and subsequently reconstituted using 20 μ l of PBS and each was assayed in duplicate. A volume of 180 μ l of substrate working solution containing 50 μ M of Succinyl-Ala-Ala-Pro-Phe-AMC (Sigma-Aldrich, St. Louis, MO, USA), was added to each well in a black 96-well plate. 10 μ l of each sample was added into the wells. Then 10 μ l of chymotrypsin working solution (1 μ g/ml) were added to each well. The rate of hydrolysis of the chymotrypsin substrate was monitored subsequently at wavelengths of 460 nm emission and 395 nm excitation, at 37 $^{\circ}$ C, by measuring the rate of increase of fluorescence in a FLUOstar OPTIMA multi-well plate reader (BMG Labtech, Ortenberg, Germany).

Identification and structural analysis of HECI. Molecular mass analysis of the contents of the HPLC fraction exhibiting maximal chymotrypsin inhibitory activity was achieved by use of an LCQ-Fleet mass spectrometer (Thermo Fisher Scientific, San Jose, CA, USA). The major peptide within this fraction was subjected, without further purification, to automated Edman degradation using an Applied Biosystems Procise 491 microsequencer (Applied Biosystems, Foster City, CA, USA) in liquid phase delivery mode. Finally, the primary structure of the novel chymotrypsin inhibitory peptide was confirmed by MS/MS fragmentation sequencing. The detection was performed in positive ion mode. The ion capillary tube was heated to 320 $^{\circ}$ C and the spray voltage was set at 4.5 kV. The MS/MS spectrum was analysed using Thermo Scientific Proteome Discoverer 1.0 software Sequest algorithm (Thermo Fisher Scientific, San Jose, CA, USA).

Molecular cloning of HECI precursor-encoding cDNA from the skin secretion cDNA library. A further 5 mg of lyophilized secretion was dissolved in lysis/binding buffer of the Dynabeads[®] mRNA DIRECT[™] Kit (DynaL Biotech Ltd., Bromborough, UK) which was used to isolate the mRNA from the secretion. The isolated mRNA was subjected to 5'- and 3'- rapid amplification of cDNA ends (RACE) procedures to obtain full-length peptide precursor nucleic acid sequence data by means of a BD SMART[™] RACE cDNA Amplification Kit (BD Biosciences Clontech, Palo Alto, CA, USA), and was further subjected to the 3'-RACE procedures using a degenerate primer (5'- GGNTGYTGGACNTTYWSNTTY-3', S = C + G; N = A + C + G + T; Y = T + C; W = A + T) that was designed to the internal amino acid sequence, -GCWTFSF-, of HECI. The 3'-RACE PCR products were purified (E.Z.N.A.[®] Cycle Pure Kit) (Omega Bio-Tek Inc., Norcross, GA, USA), and cloned using a pGEM[®]-T Easy Vector (Promega Corporation, Madison WI, USA). The nucleotide sequences of cloned cDNAs were obtained by an ABI3730 automated sequencer (Applied Biosystems, Foster City, CA, USA). Following the obtaining of the 3'-RACE product sequence, a specific antisense primer was designed to a site within the 3' non-translated region. The 5'-RACE reaction was performed by using this specific antisense primer (5'-CCACATCAGATGACTTCCTAATCAT-3') in conjunction with the UPM RACE primer. Generated PCR products were gel purified, cloned, and sequenced as described above.

Synthesis of HECI and the Lys-substituted analogue. The natural HECI (TVLRGCWTFSPFKPCI-NH₂) and the Lys-substituted analogue (K²-HECI, TVLRGCWTKSFPFKPCI-NH₂) were chemically synthesized using a solid-phase peptide synthesis approach to obtain sufficient samples for assaying bioactivities. Briefly, the Fmoc protection groups were removed by 20/80 (v/v) Piperidine/dimethylformamide (DMF, obtained from Fisher Scientific Ltd, Loughborough, UK) and the peptide bond was coupled in the presence of 2-(1H-benzotriazol-1-yl)-1,1,3,3-tetramethyluronium hexafluorophosphate (HBTU, obtained from Novabiochem[®], Darmstadt, Germany), dissolving in 11/89 (v/v) N-methylmorpholine (NMM, obtained from Fisher Scientific Ltd, Loughborough, UK)/DMF. The process employed Rink amide resin and Fmoc amino acids (Novabiochem[®], Darmstadt, Germany), and was performed in a Tribute[®] Peptide Synthesizer (Protein Technologies, Tucson, AZ, USA). The synthesized peptide was cleaved from the resin by a reaction containing 2/2/2/94 (v/v/v/v) 1,2-ethanedithiol/H₂O/thioanisole/TFA. The peptide was washed using diethyl ether and dissolved in 0.05/99.95 (v/v) TFA/water. A final concentration of 0.01% of H₂O₂ was added to perform the formation of the disulphide bond.

Determination of trypsin/chymotrypsin/human proteasome 20S inhibitory activity of HECI and the Lys-substituted analog. Phe-Pro-Arg-AMC, Succinyl-Ala-Ala-Pro-Phe-AMC and Suc-Leu-Val-Tyr-AMC (Abcam, Cambridge, UK) were used as substrates for trypsin, chymotrypsin and human 20S proteasome respectively. 10 μ l trypsin/chymotrypsin working solution (1 μ g/ml) were added to the wells of a micro-titre plate containing 180 μ l substrate and various inhibitor solutions. 10 μ l human 20S proteasome (Biochem, Boston, MA, USA) working solution (7 nM) in 50 mM HEPES buffer containing 0.035% SDS, pH 7.5 was added to the well of a micro-titre plate containing 180 μ l substrate solution and each of various inhibitor solution. Each determination was carried out in duplicate. The rate of hydrolysis of the trypsin/chymotrypsin substrate was monitored subsequently and continuously, at 37 $^{\circ}$ C, by measuring the rate of increase of fluorescence in

a FLUOstar OPTIMA multi-well plate reader (BMG Labtech, Ortenberg, Germany). For the 20 S proteasome, the rate of hydrolysis of the substrate was monitored after a pre-incubation for 15 min, at 37 °C. The inhibition curves were plotted using Morrison equation, which is showed as follow:

$$Q = K_i \times \left(1 + \frac{S}{K_m} \right) \quad (1)$$

$$y = V_0 \times \left(1 - \frac{(Et + x + Q) - \sqrt{(Et + x + Q)^2 - 4 \times Et \times x}}{2 \times Et} \right) \quad (2)$$

where, Et is the concentration of enzyme catalytic sites; S is the concentration of substrate; Km is the Michaelis-Menten constant; and V₀ is the enzyme velocity with no inhibitor. Each assay was repeated three times.

Secondary structure analyses of HECI and the Lys-substituted analogue through circular dichroism (CD). The sample peptide solutions (50 μM) were prepared in a 1 mm high precision quartz cell (Hellma Analytics, Essex, UK) by 10 mM ammonium acetate and 50% TFE in 10 mM ammonium acetate buffer respectively. CD measurements were performed at room temperature by a JASCO J-815 CD spectrometer (Jasco, Essex, UK) across the wavelength range from 190 nm–260 nm. The scanning speed was 100 nm/min, the bandwidth was 1 nm and the data pitch was 0.5 nm. The CD spectra were further analysed using the online software, BeStSel³⁵, and the following proportion of different secondary structures were predicted.

Cell viability test of peptides on cell lines. The cancer cell line H157 (ATCC-CRL-5802, ATCC, Teddington, Middlesex, UK) and PC-3 (ATCC-CRL-1435, ATCC, Teddington, Middlesex, UK) were cultured in RPMI-1640 culture medium (Invitrogen, Paisley, UK) containing 10% FBS and 1% Penicillin-Streptomycin. MCF-7 (ATCC-HTB-22, ATCC, Teddington, Middlesex, UK) was cultured in DMEM culture medium (Invitrogen, Paisley, UK) containing 10% FBS and 1% Penicillin-Streptomycin. The normal cell line HMEC-1 (ATCC-CRL-3243, ATCC, Teddington, Middlesex, UK) was cultured in MCDB131 medium (Gibco, Paisley, UK) containing 10% FBS (foetal bovine serum, obtained from Sigma-Aldrich, St. Louis, MO, USA), 1% Penicillin-Streptomycin (Invitrogen, Paisley, UK), epidermal growth factor (10 ng/mL), hydrocortisone (1 μg/mL, obtained from Sigma-Aldrich, St. Louis, MO, USA) and glutamine (10 mM). Cells were seeded into a 96-well plate and incubated for 24 h (37 °C, 5% CO₂) followed by starvation using serum-free medium. Sample solutions were loaded on this plate which was further incubated for 24 h. The 3-(4,5-dimethylthiazol-2-yl)-2,5-diphenyltetrazolium bromide (MTT) solution (5 mg/ml, 10 μl/well) was utilized to form the formazan after a 4 h incubation. Cell-produced-formazan was dissolved in DMSO (100 μl/well). The absorbance was recorded by using an ELx808™ Absorbance Microplate Reader at 570 nm (BioTek Instruments, Inc., Winooski, VT, USA). All the peptide concentrations and controls had 5 replicates in single 96-well plate and three independent experiments were performed.

Haemolysis activity test of peptides using horse erythrocytes. Completely washed horse erythrocyte (TCS Biosciences Ltd., Buckingham, UK) suspension was prepared using phosphate-buffered saline (PBS). A series of peptide solutions were incubated with a 2% suspension of red blood cells at final concentrations of 1–512 μM at 37 °C for 4 h. After the incubation, 200 μl of each supernatant was transferred into a 96-well plate and the absorbance at 550 nm was measured with a Synergy HT plate reader (BioTek Instruments, Inc., Winooski, VT, USA). The BioTek's Gen5™ software was used to analyse the result. (BioLise BioTek EL808, Winooski, VT, USA). All the peptide concentrations and controls had 5 replicates in single 96-well plate and three independent experiments were performed.

Data availability. All data generated or analysed during this study are included in this published article.

References

- Poddar, N. K., Maurya, S. K. & Saxena, V. In *Proteases in Physiology and Pathology* (eds Sajal Chakraborti & Naranjan S. Dhalla) 257–287 (Springer Singapore, 2017).
- Birk, Y. The Bowman-Birk inhibitor. Trypsin-and chymotrypsin-inhibitor from soybeans. *Chemical Biology & Drug Design* **25**, 113–131 (1985).
- McBride, J. D., Watson, E. M., Brauer, A. B., Jaulent, A. M. & Leatherbarrow, R. J. Peptide mimics of the Bowman-Birk inhibitor reactive site loop. *Peptide Science* **66**, 79–92 (2002).
- Salmon, L. *et al.* Peptide leucine arginine, a potent immunomodulatory peptide isolated and structurally characterized from the skin of the Northern Leopard frog, *Rana pipiens*. *J Biol Chem* **276**, 10145–10152 (2001).
- Wang, M. *et al.* Identification and molecular cloning of a novel amphibian Bowman Birk-type trypsin inhibitor from the skin of the Hejiang Odorous Frog. *Odorrana hejiangensis*. *Peptides* **33**, 245–250 (2012).
- Wu, Y. *et al.* A structural and functional analogue of a Bowman-Birk-type protease inhibitor from *Odorrana schmackeri*. *Bioscience reports* **37**, BSR20160593 (2017).
- Lin, Y. *et al.* pLR-HL: A Novel Amphibian Bowman-Birk-type Trypsin Inhibitor from the Skin Secretion of the Broad-folded Frog, *Hylarana latouchii*. *Chem Biol Drug Des* **87**, 91–100 (2016).
- Parlati, F. *et al.* Carfilzomib can induce tumor cell death through selective inhibition of the chymotrypsin-like activity of the proteasome. *Blood* **114**, 3439–3447 (2009).
- Song, G. *et al.* HV-BBI—a novel amphibian skin Bowman-Birk-like trypsin inhibitor. *Biochem Biophys Res Commun* **372**, 191–196 (2008).
- Prasad, E. R., Dutta-Gupta, A. & Padmasree, K. Purification and characterization of a Bowman-Birk proteinase inhibitor from the seeds of black gram (*Vigna mungo*). *Phytochemistry* **71**, 363–372 (2010).

11. Rothmund, S., Sönnichsen, F. D. & Polte, T. Therapeutic Potential of the Peptide Leucine Arginine As a New Nonplant Bowman–Birk-Like Serine Protease Inhibitor. *Journal of medicinal chemistry* **56**, 6732–6744 (2013).
12. Graham, C. *et al.* Peptide Tyrosine Arginine, a potent immunomodulatory peptide isolated and structurally characterized from the skin secretions of the dusky gopher frog. *Rana sevosia. Peptides* **26**, 737–743 (2005).
13. Catalano, M., Ragona, L., Molinari, H., Tava, A. & Zetta, L. Anticarcinogenic Bowman Birk Inhibitor Isolated from Snail Medic Seeds (*Medicago scutellata*): Solution Structure and Analysis of Self Association Behavior. *Biochemistry* **42**, 2836–2846 (2003).
14. Ho, S. & Ng, B. A Bowman-Birk trypsin inhibitor with antiproliferative activity from Hokkaido large black soybeans. *J Pept Sci* **14**, 278–282 (2008).
15. da Costa Souza, C. *et al.* Effects of an anticarcinogenic Bowman-Birk protease inhibitor on purified 20S proteasome and MCF-7 breast cancer cells. *PLoS One* **9**, e86600 (2014).
16. Chen, Y.-W., Huang, S.-C., Lin-Shiau, S.-Y. & Lin, J.-K. Bowman–Birk inhibitor abates proteasome function and suppresses the proliferation of MCF7 breast cancer cells through accumulation of MAP kinase phosphatase-1. *Carcinogenesis* **26**, 1296–1306 (2005).
17. Clemente, A., Moreno, F. J., Marín-Manzano, Md. C., Jiménez, E. & Domoney, C. The cytotoxic effect of Bowman–Birk isoinhibitors, IBB1 and IBB2, from soybean (*Glycine max*) on HT29 human colorectal cancer cells is related to their intrinsic ability to inhibit serine proteases. *Molecular nutrition & food research* **54**, 396–405 (2010).
18. Adams, J. *et al.* Proteasome inhibitors: a novel class of potent and effective antitumor agents. *Cancer research* **59**, 2615–2622 (1999).
19. Deshimaru, M., Yoshimi, S., Shioi, S. & Terada, S. Multigene family for Bowman–Birk type proteinase inhibitors of wild soja and soybean: The presence of two BBI-A genes and pseudogenes. *Bioscience, biotechnology, and biochemistry* **68**, 1279–1286 (2004).
20. Gariani, T., McBride, J. & Leatherbarrow, R. The role of the P2' position of Bowman-Birk proteinase inhibitor in the inhibition of trypsin: Studies on P2' variation in cyclic peptides encompassing the reactive site loop. *Biochimica et Biophysica Acta* **1431**, 232–237 (1999).
21. Kisselev, A. F. & Goldberg, A. L. Proteasome inhibitors: from research tools to drug candidates. *Chemistry & biology* **8**, 739–758 (2001).
22. Kisselev, A. F., Songyang, Z. & Goldberg, A. L. Why does threonine, and not serine, function as the active site nucleophile in proteasomes? *Journal of Biological Chemistry* **275**, 14831–14837 (2000).
23. Fenteany, G. *et al.* Inhibition of proteasome activities and subunit-specific amino-terminal threonine modification by lactacystin. *Science* **268**, 726–731 (1995).
24. Adams, J. The proteasome: a suitable antineoplastic target. *Nature Reviews Cancer* **4**, 349 (2004).
25. Almond, J. & Cohen, G. The proteasome: a novel target for cancer chemotherapy. *Leukemia* **16**, 433 (2002).
26. Denlinger, C. E., Rundall, B. K. & Jones, D. R. In *Seminars in thoracic and cardiovascular surgery*. 28–39 (Elsevier).
27. Fahy, B. N., Schlieman, M. G., Mortenson, M. M., Virudachalam, S. & Bold, R. J. Targeting BCL-2 overexpression in various human malignancies through NF- κ B inhibition by the proteasome inhibitor bortezomib. *Cancer chemotherapy and pharmacology* **56**, 46–54 (2005).
28. Chen, Y., Huan, S., Lin-Shiau, S. Y. & Lin, J. K. Bowman-Birk inhibitor abates proteasome function and suppresses the proliferation of MCF7 breast cancer cells through accumulation of MAP kinase phosphatase-1. *Carcinogenesis* **26**, 1296–1306 (2005).
29. Joanittl, G., Azevedo, R. & Freitas, S. Apoptosis and lysosome membrane permeabilization induction on breast cancer cells by an anticarcinogenic Bowman–Birk protease inhibitor from *Vigna unguiculata* seeds. *Cancer letters* **293**, 73–81 (2010).
30. Mangoni, M. L. *et al.* Ranacyclins, a new family of short cyclic antimicrobial peptides: biological function, mode of action, and parameters involved in target specificity. *Biochemistry* **42**, 14023–14035 (2003).
31. Raaymakers, C. *et al.* Antimicrobial peptides in frog poisons constitute a molecular toxin delivery system against predators. *Nature communications* **8**, 1495 (2017).
32. Nguyen, L. T., Haney, E. F. & Vogel, H. J. The expanding scope of antimicrobial peptide structures and their modes of action. *Trends in biotechnology* **29**, 464–472 (2011).
33. König, E., Bininda-Emonds, O. R. & Shaw, C. The diversity and evolution of anuran skin peptides. *Peptides* **63**, 96–117 (2015).
34. Goldberg, L. Functions of proteasome. *Biochemical Society* **35**, 12–17 (2007).
35. Micsonai, A. *et al.* Accurate secondary structure prediction and fold recognition for circular dichroism spectroscopy. *Proceedings of the National Academy of Sciences* **112**, E3095–E3103 (2015).

Author Contributions

The conception and design of study was conducted by Lei Wang, Mei Zhou and Tianbao Chen. The laboratory work and acquisition of data was performed by Luyao Zhang, Xiaoling Chen, and Yue Wu. The analysis of data was conducted by Chengbang Ma, Xinping Xi and Luyao Zhang. Drafting of article was written by Luyao Zhang, Xiaoling Chen and Mei Zhou and final approval of manuscript was revised by Brian Walker, Tianbao Chen and Chris Shaw.

Additional Information

Competing Interests: The authors declare no competing interests.

Publisher's note: Springer Nature remains neutral with regard to jurisdictional claims in published maps and institutional affiliations.



Open Access This article is licensed under a Creative Commons Attribution 4.0 International License, which permits use, sharing, adaptation, distribution and reproduction in any medium or format, as long as you give appropriate credit to the original author(s) and the source, provide a link to the Creative Commons license, and indicate if changes were made. The images or other third party material in this article are included in the article's Creative Commons license, unless indicated otherwise in a credit line to the material. If material is not included in the article's Creative Commons license and your intended use is not permitted by statutory regulation or exceeds the permitted use, you will need to obtain permission directly from the copyright holder. To view a copy of this license, visit <http://creativecommons.org/licenses/by/4.0/>.

© The Author(s) 2018